Applied Catalysis B: Environmental 123–124 (2012) 357–366

Contents lists available at SciVerse ScienceDirect

Applied Catalysis B: Environmental

journal homepage: www.elsevier.com/locate/apcatb

# Deoxygenation of benzofuran in supercritical water over a platinum catalyst

Jacob G. Dickinson, Jack T. Poberezny, Phillip E. Savage*

*Department of Chemical Engineering, University of Michigan, Ann Arbor, MI 48109-2136, USA*

ARTICLE INFO

*Article history:*
Received 12 March 2012
Received in revised form 26 April 2012
Accepted 1 May 2012
Available online 10 May 2012

*Keywords:*
Hydrothermal
Hydrodeoxygenation
Kinetics
Benzofuran
Pt/C

ABSTRACT

This study reports the results of the catalytic deoxygenation of 2,3-benzofuran in supercritical water over a 5 wt% platinum on activated carbon catalyst. We examine the effect of batch-holding time, water loading, hydrogen loading, and catalyst loading on the reaction products. The major products were 2-ethylphenol, ethylbenzene, ethylcyclohexanone, ethylcyclohexanol, and ethylcyclohexane. Increasing the water loading or decreasing the hydrogen loading decreases the selectivity to aromatic deoxygenated products (e.g. ethylbenzene) and increases the selectivity to hydrogenated deoxygenated products (e.g. ethylcyclohexane). Combining the results from these benzofuran experiments with results obtained in separate experiments with the above-mentioned reaction products as the starting reagent allowed for the development of the hydrothermal deoxygenation reaction network. The reaction network provided a foundation for a quantitative kinetic model that correlated the experimental results. The model showed that the experimental results were consistent with benzofuran having an inhibitory effect on the deoxygenation of ethylphenol to ethylbenzene.



## 1. Introduction

Second generation biofuels produced from microalgae have shown great promise due to microalgae's high growth rate, ability to grow in a variety of water sources, and limited fuel versus food controversy. Unfortunately, microalgae grow as a dilute suspension in water, making conventional technologies for conversion of dry biomass, such as pyrolysis and transesterification, impractical due to the large energy input needed to vaporize water. These factors motivate research into the processing of wet microalgae through, for example, hydrothermal liquefaction.

Hydrothermal liquefaction treats biomass at high temperatures (200–400 °C) and pressures (1.5–22 MPa) to break down macromolecules into smaller, liquid-fuel-range molecules. Using reactor pressures at or above the saturation pressure ensures that the water remains in the liquid phase, below the critical point, allowing for heat to be efficiently recovered post liquefaction. The organic product from this reaction, often called bio-crude, is high in nitrogen (5–7 wt%) and oxygen (5–20 wt%) [1–11]. Removal of these heteroatoms is essential for the production of clean liquid fuels compatible with the current energy infrastructure.

Removal of heteroatoms can be accomplished by conventional hydrotreating upon the separation of the bio-crude from the water. Recent work has shown that this separation is not trivial for some algae species because the high heteroatom content in the bio-crude results from hydrophilic functional groups (carboxylic acids, alcohols, and amines) that can create an oil/water emulsion [2,10,11]. Furthermore, the aqueous reactor effluent may contain functionalized organics that could be used in fuels, and, if left in the aqueous phase, could require significant wastewater treatment. Therefore, catalytic processing of the bio-crude and aqueous streams together could have engineering advantages for producing liquid fuels via hydrothermal liquefaction.

Catalytic processing of biomass and bio-crudes to produce liquid fuels in a hydrothermal environment has recently received attention. Below we examine representative research.

In a series of studies, Duan and Savage reduced the nitrogen and oxygen content and produced a freely flowing bio-oil by upgrading algal bio-crude in supercritical water ($T \geq 374$ °C, $P \geq 3190$ psig (22 MPa)) using Pt/C and Pd/C catalysts [12–14]. They also found that direct catalytic liquefaction using a variety of supported metal catalysts (Pt/C, Pd/C, Ru/C, $CoMo/Al_2O_3$, $Ni/SiO_2Al_2O_3$) was effective at increasing the yield of algal bio-crude [3]. Similarly, Kunkes et al. converted sorbitol into monofunctional hydrophobic liquid hydrocarbons over a PtRe/C catalyst between 210 and 250 °C without added hydrogen. They speculated that the PtRe/C catalyst, which was stable for at least 1 month, reformed a small portion of the sorbitol to produce the hydrogen necessary for the subsequent deoxygenation reactions [15]. In a similar study, Vispute et al. produced commodity chemicals (benzene, toluene, ethylbenzene, and ethylene) from the aqueous phase processing of water-soluble pyrolysis oil over Ru/C, Pt/C, and zeolite catalysts with added hydrogen [16,17].

* Corresponding author at: 3074 H.H. Dow Building, 2300 Hayward Street, Ann Arbor, MI 48109, USA. Tel.: +1 734 764 3386; fax: +1 734 763 0459.
*E-mail address:* psavage@umich.edu (P.E. Savage).

0926-3373/$ – see front matter © 2012 Elsevier B.V. All rights reserved.
http://dx.doi.org/10.1016/j.apcatb.2012.05.005

The above reports illustrate that a hydrothermal environment can be effectively used to upgrade biomass feedstocks to fuels, but they provide limited knowledge about the interactions of the molecules and the catalyst surface, and the associated reaction kinetics. For a more detailed understanding of these reactions, model compound studies have been employed. Several authors have identified free fatty acids and heterocyclic nitrogen compounds as the main carriers of heteroatoms in algal bio-crude [1,2,8,10,11]. Free fatty acids account for approximately one third of the oxygen in the bio-oil from algae liquefaction [2,10]. In addition to free fatty acids, phenolic and furanic compounds have also been identified [5], and likely account for the remaining oxygen content. Furanic compounds have also received significant attention in non-aqueous environments because they are commonly found in biofuels derived from lignocellulosic biomass [18].

There have been limited studies on hydrothermal catalytic heteroatom removal from model compounds. Duan and Savage found that using supercritical water as a reaction medium changed the reaction pathways for the hydrodenitrogenation of pyridine over a Pt/C catalyst, indicating that studies performed in a conventional hydrotreating environment may not be applicable to those carried out in a hydrothermal environment [19]. Fu et al. found that Pt/C was an effective catalyst for the decarboxylation of free fatty acids in sub- and supercritical water and suffered no significant change in activity through three consecutive 3 h reactions at 370 °C [20,21]. Interestingly, the decarboxylation occurred without the addition of hydrogen to the reaction. This result led to speculation that under these conditions, water may donate hydrogen to the reactions. To the best of our knowledge, there has not been a detailed study of reaction kinetics or the influence of process variables on the catalytic deoxygenation of furans or phenols in sub- or supercritical water.

To fill this knowledge gap, we chose 2,3-benzofuran as a model heterocyclic compound. Previous studies in non-aqueous environments suggest that benzofuran deoxygenates through a pathway that includes phenols and alcohols, which, as we will show, led us to insights about the effects of having these various species all present in the reaction [22–25]. We report herein a reaction network and the kinetics of deoxygenation, both of which are essential to the design of future catalytic processes. Experiments and kinetic modeling were accomplished over a wide range of conversions and yields of deoxygenated products to provide industrially relevant information. We also report on the process variables that affect reaction rate and selectivity. Selectively producing aromatic deoxygenated products instead of hydrogenated deoxygenated products was desired to minimize hydrogen consumption.

## 2. Materials and methods

All solvents and reagents were obtained from Sigma–Aldrich in high purity (≥99%) and used as received. Platinum on activated carbon (5 wt%) was also obtained from Sigma–Aldrich and was used without prior reduction. Batch reactors constructed from a 1/2 in. Swagelok port connector, cap, and 1/2 to 1/8 in. reducing union were fitted with 9 in. of 1/8 o.d. stainless steel tubing and a 30,000 psi High Pressure Equipment Company valve. The assembled reactors had a nominal volume of 4.1 mL. Prior to use in reactions, all reactors were loaded with 2 mL of deionized water and heated to 350 °C for 60 min to expose the reactor walls to a hydrothermal environment.

Unless otherwise specified, 10 mg of 5 wt% Pt/C, 100 μL (900 μmol) of benzofuran (or the molar equivalent of ethylcyclohexanol, ethylcyclohexane, ethylbenzene, or ethylphenol), and 0.67 mL deionized water were loaded into each reactor. After loading the catalyst and liquid reagents, we sealed the reactors and connected them to a gas manifold that included hydrogen and helium cylinders and a vacuum pump. Air was removed from the reactors by 4 cycles of helium pressurization (50 psig) followed by evacuation by the vacuum pump (1.5 psia). On the last cycle, we placed 77 psig of helium into the reactor to act as an internal standard, followed by final pressurization with hydrogen to achieve the desired nominal hydrogen to reactant molar ratio (0:1, 0.5:1, 2:1, 3:1, 4:1, and 6:1). The hydrogen to reactant ratios were chosen to be moderately substoichiometric with respect to producing ethylcyclohexane through deoxygenation and hydrogenation reactions, with the exception of the 6:1 hydrogen to benzofuran reactions, which were stoichiometric. The tables in Supplementary data provide the exact hydrogen pressures for each reaction. The reactors were checked for leaks during this pressurization by placing them in water.

A preheated Techne Fluidized Sand Bath (model SBL-2) with a Techne TC-8D temperature controller heated the reactors to the desired temperature in approximately 2 min. We started a reaction timer when the reactors were placed in the sandbath. The reactors were continuously agitated using a wrist-action shaker set to 1° of rotation. After the desired time, the reactors were removed from the sand bath, quenched in water at room temperature, and allowed to equilibrate at room temperature for at least 120 min. Gas analysis was performed at this point using a Agilent 6890N gas chromatograph with a thermal conductivity detector (GC-TCD) and the chromatographic procedure outlined by Brown et al. [2]. We then purged the remaining gas and opened the reactors. The reaction products were extracted by repeatedly rinsing the reactor body and valve assembly with acetone until a 10 mL volumetric flask was filled. The reaction products were centrifuged at 3200 relative centrifugal forces for 3 min to facilitate the catalyst removal.

We identified the reaction products in the acetone solution using an Agilent 6890N gas chromatograph with a mass spectrometric detector (GC-MSD) and a HP-5MS capillary column. Complete separation of all products was observed by injecting 2 μL of the extracted reaction product solution into an inlet at 310 °C with a 50:1 split ratio and helium flowing at 1 mL/min as the carrier gas. The column was initially held at 50 °C for 4 min, then ramped at 2 °C/min to 110 °C, 10 °C/min to 160 °C, and 25 °C/min to 300 °C where the temperature was held for 3 min. Quantification of compounds identified using the GC-MSD was carried out on a Agilent 6890 GC with a flame ionization detector (GC-FID) using the same method described above. Response factors for compound quantification were determined by analyzing standard solutions of the identified compounds in known concentrations. Yields are calculated throughout using the following equation:

$$\text{Yield} = \frac{\text{mol C in product}}{\text{mol C loaded into reactor}} \quad (1)$$

We performed parameter estimation and solved the differential equation kinetic model using Matlab® and the optimtool package. A variety of kinetic models were proposed and fit. The ability of the models to fit the data was compared based on the minimized error between the model and experimental concentrations, $C_i$, as shown below, and the absence of systematic deviations in parity plots.

$$\text{Error} = \sum_i (C_{i,\text{Data}} - C_{i,\text{model}})^2 \quad (2)$$

## 3. Results and discussion

This section provides information about control experiments, reaction products, the reaction network, and reaction kinetics. We first discuss the experiments performed to ensure that the chemical transformations observed were due to the presence of the platinum catalyst and to quantify the mass losses from the

laboratory procedures. The second section reports the identities and yields of the reaction products and the effect of process variables. We performed replicate experiments and report the mean values along with the standard deviation as an estimate of the uncertainty. The third section provides a reaction network deduced from the results from reacting benzofuran, reaction intermediates, and reaction products. Finally, we use the network and experimental data to develop a kinetic model.

### 3.1. Control experiments

To determine the amount of organic material lost during air evacuation, sample workup, and adsorption to the Pt/C, three reactors were loaded, purged, pressurized, agitated for one hour at room temperature, and extracted using the procedure outlined in the Materials and Methods section. Quantification of the recovered benzofuran using GC-FID indicated that $849 \pm 36$ μmol of the original 900 μmol benzofuran was recovered. Similarly, control experiments with reactors loaded with ethylphenol and ethylcyclohexanol had recoveries of $802 \pm 22$ and $865 \pm 18$ μmol, respectively, of the original 900 μmol. The high viscosity of ethylphenol made fully loading the reactors difficult, and this led to the lower carbon recovery. These values were used to determine that the average recovery of carbon from the reactors was greater than 94% for all reactions where the starting reagents were benzofuran, ethylphenol, or ethylcyclohexanol. The recovered amounts of benzofuran, ethylphenol, and ethylcyclohexanol were used to compute the initial concentrations of the starting reagents.

We performed a set of uncatalyzed reactions to be certain that the chemical transformations were due to the presence of the Pt/C catalyst. A benzofuran reaction at 450 °C for 60 min with a 5:1 hydrogen to benzofuran molar ratio showed the presence of no deoxygenated products and a conversion of less than 10%.

### 3.2. Reaction products

GC-MSD and GC-TCD analysis identified numerous liquid- and gas-phase products from reacting benzofuran over the 5 wt% Pt/C catalyst at 380 °C. These included liquid-phase oxygenated products (2-ethylphenol, 2-ethylcyclohexanone, 2-ethylcyclohexanol, 2-methylphenol, and phenol), liquid-phase deoxygenated products (ethylbenzene, ethylcyclohexane, toluene, benzene, and heptane), and gas phase products (ethane, methane, hydrogen, and carbon dioxide). This section shows how process variables such as batch holding time, water density, hydrogen loading, and catalyst loading affect the concentrations of the products. With the knowledge obtained from these experiments, we later develop a reaction network and kinetic model.

#### 3.2.1. Influence of batch holding time

Figs. 1 and 2 show the effect of reaction time on the concentration of the major products from the hydrothermal catalytic deoxygenation of benzofuran at two different hydrogen to benzofuran molar ratios. The large symbols on the figures represent the experimental data and the curves, with the corresponding smaller symbols, represent model results. The kinetic model will be discussed in Section 3.4. In this section we confine the discussion to the trends evident in the experimental data.

Figs. 1 and 2 show that the benzofuran concentration rapidly decreases with time. Conversions of $89 \pm 2$% and $95 \pm 3$% were obtained in 10 min with the 4:1 and 6:1 ratios, respectively. The concentration of ethylphenol increased rapidly as benzofuran was consumed, reaching a maximum of approximately 0.13 and 0.08 M for the 4:1 and 6:1 reactions, respectively. The reasons for the differences in concentrations of the reaction products at the two different hydrogen loadings will be discussed in Section 3.2.3. After reaching a maximum value between 10 and 15 min, the concentration of ethylphenol decreases approximately linearly. The experimental data in Fig. 2 indicate that at a 6:1 hydrogen to benzofuran molar ratio, the concentrations of ethylcyclohexanone and ethylcyclohexanol reach a maximum (0.03 M) at 10 min before decreasing. Only low (<0.008 M) concentrations of ethylcyclohexanone and ethylcyclohexanol were observed at the lower hydrogen loading (Table S1, supplementary information), therefore these products were considered minor for this reaction. The reason for the distinction between minor and major products and the causes of this distinction will be discussed later.

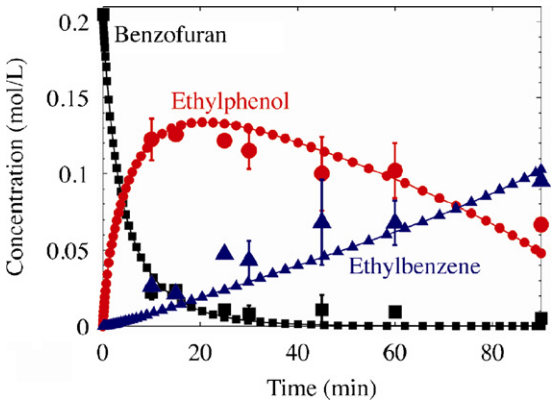


**Fig. 1.** Major products from benzofuran at 380 °C with a 4:1 hydrogen to benzofuran molar ratio.

Figs. 1 and 2 indicate that ethylbenzene was the major deoxygenated product at both reaction conditions. Both figures show that the concentration of ethylbenzene increases approximately linearly with time. The concentration of ethylbenzene at 60 min is nearly identical for both reactions with values of $0.07 \pm 0.01$ and $0.083 \pm 0.007$ M for the 4:1 and 6:1 reactions, respectively. In addition to ethylbenzene, ethylcyclohexane was observed at the higher hydrogen loading. Similar to ethylbenzene, the concentration of ethylcyclohexane increased nearly linearly for the reaction times studied.

These observations provide significant insight into the reaction network of benzofuran. The high concentration of ethylphenol

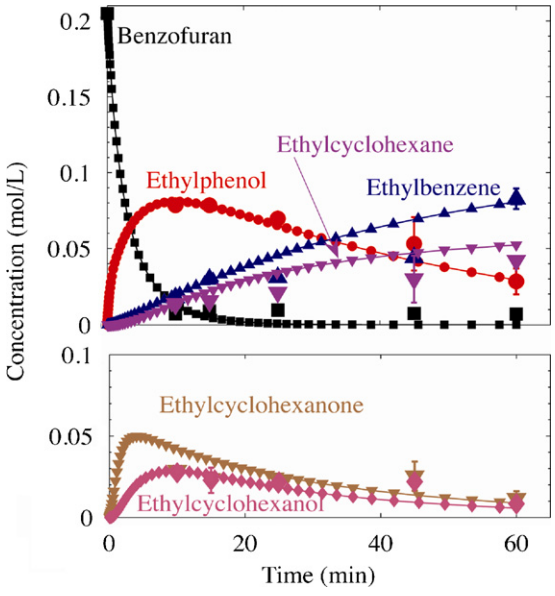


**Fig. 2.** Major products from benzofuran at 380 °C with a 6:1 hydrogen to benzofuran molar ratio.

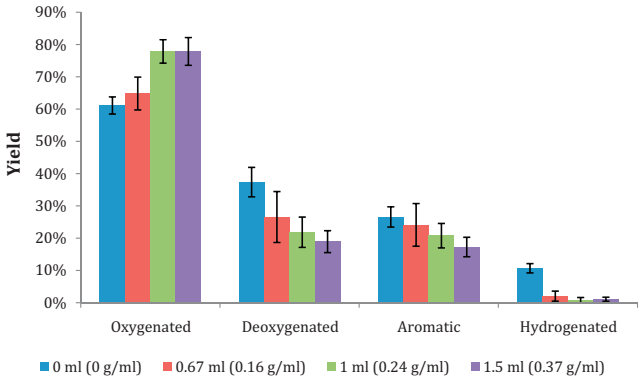


**Fig. 3.** Effect of water loading on the product distribution from benzofuran at 380 °C for 30 min with a 4:1 hydrogen to benzofuran ratio. The water densities at the reaction conditions are listed in parentheses. The aromatic and hydrogenated products are the two classes of deoxygenated products.

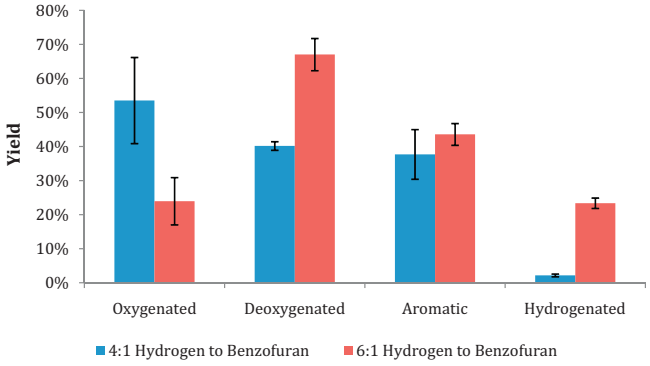


**Fig. 4.** Product yields from reacting benzofuran with hydrogen at 4:1 and 6:1 molar ratios at 380 °C, 60 min.

in Figs. 1 and 2, and this concentration passing through a maximum before declining, indicates that ethylphenol is a major reaction intermediate for benzofuran deoxygenation. Fig. 2 indicated that ethylcyclohexanone and ethylcyclohexanol also passed through maximum concentrations, again suggesting that these products were intermediates in the deoxygenation of benzofuran. Figs. 1 and 2 also showed that the concentrations of ethylbenzene and ethylcyclohexane continuously increased under the conditions studied. This behavior suggests that these are the terminal products of the reaction. The full reaction network will be discussed in detail in Section 3.3.

### 3.2.2. Influence of water density

Previous work on hydrothermal catalytic denitrogenation indicates that catalytic reaction pathways and selectivities can be altered when the reactions are conducted in water [19]. Fig. 3 shows the effect of water loading on the product yields. It should be noted that for all of these reactions the amounts of Pt/C (10 mg), benzofuran (900 μmol), helium (77 psig at 25 °C), and hydrogen (350–400 psia at 25 °C) were fixed so all the reactors had the same concentrations of hydrogen, benzofuran, and catalyst. The reactors had different pressures, however, due to the different water loadings. We estimate the pressures to be 870, 4000, 4100, and 4200 psig, respectively.

Fig. 3 and Table S2 indicate that as the water density increases, the yield of deoxygenated products decreases whereas the yield of oxygenated products increases. Furthermore, the distribution of deoxygenated products, designated as aromatic and hydrogenated, changes significantly as more water is added. With no water present, the yields of hydrogenated and aromatic products were 11 ± 1% and 27 ± 3%, respectively. At a water density of 0.16 g/mL, the yield of hydrogenated products decreases dramatically to 2 ± 2%, whereas the yield of aromatic products, 24 ± 7%, shows little change. Increasing the water density further has little effect on the yield of hydrogenated products, but the yield of aromatic products decreases. These results indicate that water density can be used to alter the selectivity to deoxygenated products and their extent of hydrogenation.

The reason for the decrease in deoxygenated product yield (undesired) and in selectivity toward hydrogenated products (desired) with increasing water concentration is not clear at present. We suspect that competitive binding of water to the platinum surface might play a role. The presence of water on the catalyst surface would reduce the number of sites available for benzofuran and hydrogen, thereby reducing the rates for both deoxygenation and hydrogenation of the oxygenated products. Fig. 3 showed that the presence of water has a larger influence on hydrogenation than deoxygenation. This result is likely related to multiple surface bound hydrogen atoms being needed to fully hydrogenate the molecule. The presence of water may decrease the likelihood of bound hydrogen atoms interacting with the bound aromatic molecule to hydrogenate it. From a rate law perspective, this suggests that the rate of hydrogenation is more dependent on the hydrogen concentration than is the rate of deoxygenation.

### 3.2.3. Influence of hydrogen loading

Fig. 4 shows that the initial amount of hydrogen loaded into each reactor had a large effect on product yields from benzofuran. Increasing the hydrogen loading from 4:1 to 6:1 increased the yield of hydrogenated products at 60 min from 2.2 ± 0.4 to 23 ± 2%, decreased the yield of oxygenated products from 54 ± 13 to 24 ± 7%, but had no significant effect on the yield of aromatic products (38 ± 7 and 44 ± 3%, respectively). The absolute increase in yield of hydrogenated products with the 6:1 hydrogen to benzofuran molar ratio is about the same as the increase in the yield of deoxygenated products and decrease in yield of oxygenated products. The ten-fold relative increase in yield of hydrogenated products, which greatly exceeds the 70% relative increase in yield of deoxygenated products, suggests that the rate of the hydrogenation pathway has a higher hydrogen reaction order than does the direct deoxygenation pathway, which produces aromatic products. Recall that the experimental data in the previous section also suggested a higher hydrogen order for the hydrogenation pathway. The increase in the yield of hydrogenated products was also accompanied by an increase in the amount of hydrogen consumed per molecule of benzofuran at 60 min (2.4 ± 0.3 to 2.8 ± 0.1, respectively).

The influence of hydrogen on the reaction is also apparent in Figs. 1 and 2. Both conditions resulted in the rapid conversion of benzofuran, but the 4:1 reaction produced a higher concentration of ethylphenol (0.12 ± 0.01 M) than the 6:1 reaction (0.08 M). The higher concentration of ethylphenol in the 4:1 reaction is likely a result of slower hydrogenation of the ethylphenol at the lower hydrogen loading. This hypothesis is supported by ethylcyclohexanone and ethylcyclohexanol being present in lower concentrations at the 4:1 hydrogen to benzofuran ratio (0.008 M, maximum for each) than at the 6:1 ratio (0.03 M, maximum for each) as shown in Table S1 and Fig. 2. The combined concentrations of ethylphenol, ethylcyclohexanone, and ethylcyclohexanol are similar for both reaction conditions at 10 min (Table S1).

Gas analysis, shown in Table 1, indicated that the reaction produced primarily carbon dioxide. Methane and ethane were also present, but in approximately 10–20% of the quantity of carbon dioxide. Overall, the yield of carbon-containing gases was

**Table 1**
Gases produced 380 °C, 60 min.

| | $CO_2$ (μmol) | $CH_4$ (μmol) | $C_2H_6$ (μmol) | Total yield (%) |
|---|---|---|---|---|
| 4:1 Hydrogen:Benzofuran | 96 ± 6 | 14 ± 6 | 7.3 | 1.6 ± 0.1 |
| 6:1 Hydrogen:Benzofuran | 87 ± 4 | 5.5 ± 0.3 | 0 | 1.36 ± 0.07 |

approximately 1.5% for both the 4:1 and 6:1 hydrogen to benzofuran ratios. Table 1 indicates that the amount of carbon dioxide produced is similar for both conditions, but the amounts of methane and ethane decrease with increasing hydrogen concentration. The increase in methane and ethane production at lower hydrogen concentrations suggests that hydrogen suppresses cracking reactions. The similar concentrations of carbon dioxide are likely because carbon dioxide can be produced upon oxidation of the catalyst support [26].

### 3.2.4. Influence of catalyst loading

Fig. 5 and Table S3 show the results from the hydrothermal catalytic deoxygenation of benzofuran with 5 and 10 mg loadings of Pt/C. The yield of deoxygenated products was much lower at the lower catalyst loading. This decrease in deoxygenated products was accompanied by only a modest decrease in the conversion of benzofuran (89 ± 2% with 10 mg of Pt/C, 83% with 5 mg of Pt/C). This result confirms that benzofuran conversion is faster than deoxygenation. The deoxygenated products at both catalyst loadings consisted almost entirely of aromatic products, and both catalyst loadings produced about the same yield of hydrogenated products. These results show that adding more catalyst increases the selectivity of deoxygenated products and decreases the selectivity of oxygenated products. This change in selectivity provides further evidence that the oxygenated products are reaction intermediates and the deoxygenated products are terminal products, because increasing the catalyst loading increases the reaction rate causing the reaction to move more toward completion.

## 3.3. Reaction network

The results presented in the previous sections provided numerous insights into the reaction network for benzofuran deoxygenation. Recall that ethylbenzene and ethylcyclohexane were terminal reaction products because their concentrations continuously increased with time. Ethylphenol, ethylcyclohexanone, and ethylcyclohexanol were intermediate products because their

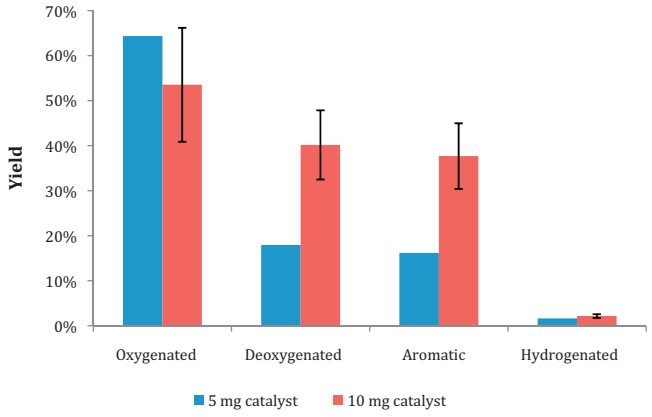


**Fig. 5.** Product yields from benzofuran with hydrogen at a 4:1 molar ratio at 380 °C, 60 min with 5 or 10 mg of 5 wt% Pt/C.

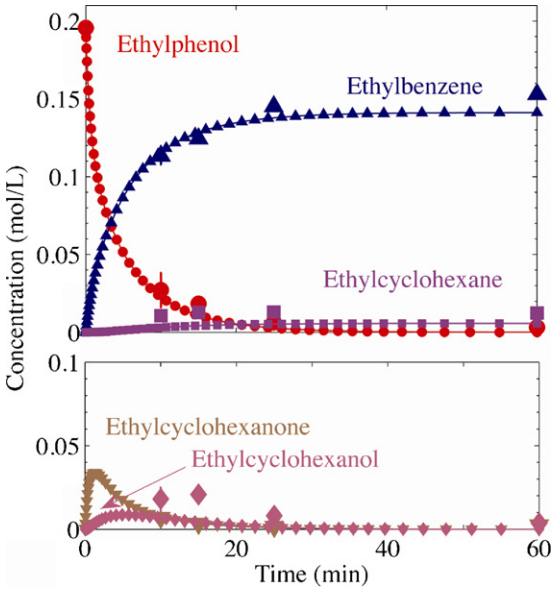


**Fig. 6.** Major products from ethylphenol at 380 °C with a 3:1 hydrogen to ethylphenol molar ratio.

concentrations passed through a maximum as time increased. This section provides results from experiments with each of these products as the starting material. These results ultimately lead to the construction of a complete reaction network for the hydrothermal catalytic deoxygenation of benzofuran.

Reacting hydrogen and ethylbenzene in supercritical water in a 2:1 molar ratio produced only ethylcyclohexane. The hydrogenation of ethylbenzene occurred rapidly and reached equilibrium in less than 10 min at 380 °C (Table S1). At equilibrium, the yield of ethylcyclohexane was 43 ± 4%. Reacting ethylcyclohexane without hydrogen for 15 min produced a 43% yield of ethylbenzene (Table S1). These results indicate that ethylbenzene and ethylcyclohexane are linked by a reversible hydrogenation/dehydrogenation reaction. Also, the absence of phenols, alcohols, and ketones in these experiments provided evidence that any hydrogenolysis reactions that remove oxygen atoms as water, to produce ethylbenzene or ethylcyclohexane, are irreversible.

Fig. 6 shows the results from experiments starting with ethylphenol and a 3:1 hydrogen to ethylphenol molar ratio. The first data point, taken at 10 min, shows ethylbenzene and ethylcyclohexane concentrations that correspond to a 64 ± 2% yield of deoxygenated products. This result represents a significant increase in the rate of deoxygenation when compared to either benzofuran reaction (Figs. 1 and 2), where the maximum yield of deoxygenated products was just 17% at 10 min. Of the deoxygenated products, 86% are aromatic, while 14% are hydrogenated. Ethylbenzene was the major reaction product. This result indicates that ethylbenzene is likely formed directly from ethylphenol. Smaller amounts of ethylcyclohexane, ethylcyclohexanone, and ethylcyclohexanol also formed. Hydrogenation of ethylphenol must be responsible for the presence of ethylcyclohexanone and ethylcyclohexanol. We hypothesize that ethylcyclohexanone was first produced from ethylphenol, followed by a rapid hydrogenation to ethylcyclohexanol. We determined that the hydrogenation reactions for ethylphenol and ethylcyclohexanone are reversible by finding that ethylcyclohexanol produced ethylcyclohexanone and ethylphenol, as shown in Fig. 7. We also propose that ethylcyclohexane is produced by the irreversible elimination of the hydroxyl group in ethylcyclohexanol.

The ratio of the concentration of ethylbenzene to ethylcyclohexane at 25 min varied with the starting reagent. Starting with

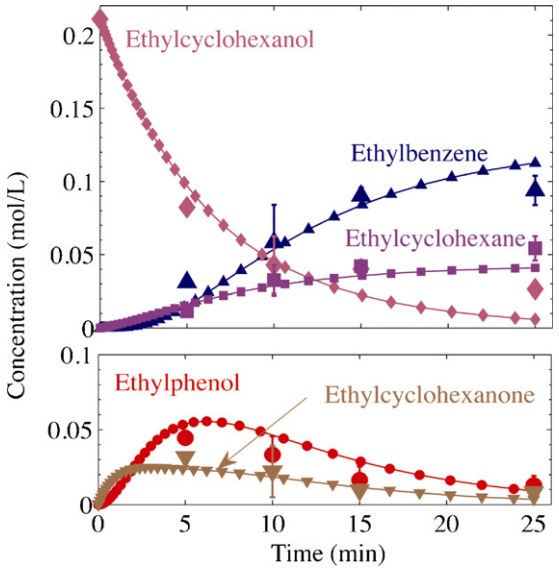


**Fig. 7.** Major products from ethylcyclohexanol at 380 °C with a 0.5:1 hydrogen to ethylcyclohexanol molar ratio.

ethylphenol (Fig. 6), ethylcyclohexanol (Fig. 7), and benzofuran (6:1, Fig. 2) resulted in ethylbenzene to ethylcyclohexane ratios of 11, 1.7, and 1.5, respectively (see Table S1 for concentration data). The much higher ratio for experiments starting with ethylphenol led us to speculate that ethylphenol inhibits the reversible hydrogenation of ethylbenzene to ethylcyclohexane. To test this hypothesis we reacted ethylbenzene and 2-methylphenol (1:1 molar ratio, 450 μmol each) in supercritical water. We chose methylphenol as an ethylphenol analog, because it produces toluene, not ethylbenzene, upon deoxygenation, allowing us to distinguish between the products from the two starting reagents. This reaction produced significantly less ethylcyclohexane than when we started with pure ethylbenzene and hydrogen (Table S4). At 10 min, with a 2:1 hydrogen to organic reagent molar ratio, the ethylbenzene and methylphenol reaction produced only 37 μmol of ethylcyclohexane while 377 μmol of ethylbenzene remained. From these values we calculate a yield of ethylcyclohexane from ethylbenzene of 8%. This yield represents a significant retardation in ethylbenzene hydrogenation when compared to the 43% yield of ethylcyclohexane formed when pure ethylbenzene was reacted. This result indicates that in the presence of ethylphenol, the hydrogenation/dehydrogenation of ethylbenzene and ethylcyclohexane are not major reactions. No previous researchers have noted such an effect.

The inhibition of ethylbenzene hydrogenation in the presence of ethylphenol may be due to ethylphenol adsorbing more strongly than ethylbenzene on the catalyst surface. Some oxygenated aromatics (i.e. acetophenone) can have significantly higher adsorption energies than benzene on Pd [27]. A higher heat of adsorption for the oxygenated species means it is likely to be more dominant on the catalyst surface.

Experiments with benzofuran as the starting reagent gave dihydrobenzofuran in small quantities (<6% yield) at short reaction times (<30 min). The rapid appearance of ethylphenol and very low concentration of dihydrobenzofuran suggests that after benzofuran is hydrogenated to dihydrobenzofuran, hydrogenolysis of the furan ring rapidly produces ethylphenol. Fig. 8 summarizes the major reaction pathways outlined above.

In addition to the major pathways, a set of minor pathways led to less abundant products such as phenol, 2-methylphenol, toluene, benzene, and heptane. Reactions of benzofuran produced maximum yields of each of 0.8, 2.5, 3.5, 2.0, and 2.3%, respectively. Experiments starting with ethylphenol or ethylcyclohexanol produced maximum heptane yields of 5.5 and 3.9%, respectively. In general, the average yield of minor products was similar when ethylphenol (5 ± 1%), ethylcyclohexanol (3 ± 3%), and benzofuran (6 ± 1%, 4:1 and 4 ± 1%, 6:1) were the starting reactants.

The low concentrations of these products permit only a speculative discussion of their reaction pathways. Heptane could be formed by a partial hydrogenation of the aromatic ring in ethylphenol, hydrogenolysis of the ring and hydroxyl group, and hydrogenation of any remaining double bonds. Methylphenol is likely produced from the hydrogenolysis of the carbon-carbon bond in the ethyl group on ethylphenol. Hydrogenolysis of the hydroxyl group on the resulting methylphenol molecule then produces toluene. Further hydrogenolysis of the methyl substituent on methylphenol could produce phenol, which then produces benzene through hydrogenolysis of the hydroxyl group. It is unlikely that the hydrogenolysis of ethylbenzene produced toluene and benzene, because these products were not observed when pure ethylbenzene was reacted. A direct reaction path between ethylphenol and phenol is supported by the presence of ethane in the gas product.

Fig. 8 shows the major and minor reaction pathways discussed above. This reaction network is similar to those previously proposed for non-hydrothermal conditions with the exception of the inclusion of ethylcyclohexanone and exclusion of molecules where the aromatic ring is only partially hydrogenated [22–25,28].

### 3.4. Reaction kinetics

Having established a reaction network for benzofuran deoxygenation, we next used the major reaction pathways as the basis for a kinetics model. Fig. 8 defines the subscript for each concentration variable and the associated rate constants.

#### 3.4.1. Model definition

The model is a set of differential equations (Table 2) resulting from combining the batch reactor design equation with rate equations for the major reaction paths. The reaction orders for each reaction follow the reaction stoichiometry with the exception of reaction (1). Here we assume that $k_a$ is essentially instantaneous because of the very low concentration of dihydrobenzofuran in the reaction products, and thus take $k_1$ to be the rate constant for both the hydrogenation of benzofuran and the hydrogenolysis of dihydrobenzofuran. Fitting the temporal variations of the species' concentrations from the experiments with each of the different starting reagents (i.e. benzofuran, ethylphenol, and ethylcyclohexanol) separately revealed that each of the rate constants was of similar magnitude, regardless of the starting reagent, with the exception of $k_2$. As noted in Section 3.3, when the starting reactant was benzofuran, reaction (2) (Fig. 8) was significantly slower than when starting with ethylphenol or ethylcyclohexanol. This lower value for $k_2$ indicates that benzofuran inhibited this reaction. This inhibition by benzofuran has also been observed with a $CoMo/Al_2O_3$ catalyst [24]. In addition to this reaction, we also noted in Section 3.3 that the minor product yields were similar for all of the starting reagents even though ethylphenol was present in greater concentrations for longer times when benzofuran was the starting reagent. This observation suggests that the rate of minor product formation is faster without benzofuran present, implying that benzofuran inhibits this lumped reaction. To account for this inhibition, we included a "$1 + K_{BF}C_{BF}$" term in the denominators of the rate equations for the direct deoxygenation pathway (reaction (2), Fig. 8) and the lumped minor products pathway (reaction (6), Fig. 8). Furthermore, to improve the accuracy of this model, we used a linear fit of the experimental benzofuran concentration data for times greater than zero to calculate the benzofuran concentration in the "$1 + K_{BF}C_{BF}$" denominator.

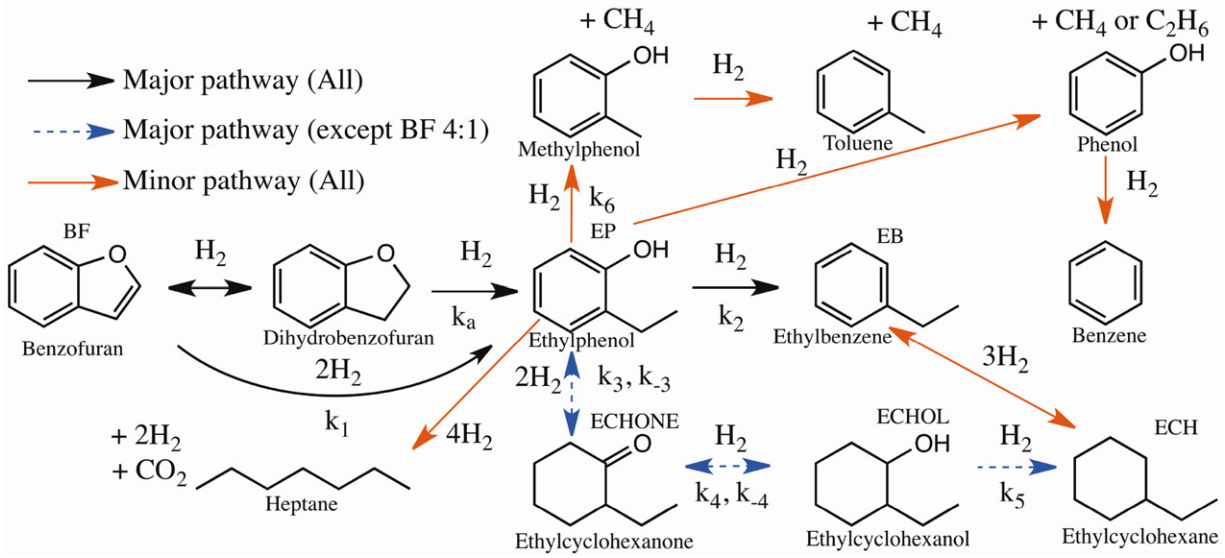


**Fig. 8.** Proposed reaction network for benzofuran deoxygenation in supercritical water at 380 °C.

We speculate that the physical basis for this inhibition is that benzofuran blocks the active site for the direct deoxygenation of ethylphenol, while leaving the active sites for other reactions unaffected. It is puzzling that a similar decrease in the rate of ethylphenol hydrogenation to ethylcyclohexanone did not occur, but its absence may be because the hydrogenation and hydrogenolysis reactions occur at different active sites.

### 3.4.2. Kinetic parameters

Table 3 shows the optimized values for the eight reaction rate constants and the benzofuran adsorption equilibrium constant ($K_{BF}$). To aid in the discussion of these rate constants, we also define the effective $k_2$, $k_{2,eff}$, as $k_2/(1+K_{BF}C_{BF})$. An optimized value of 965 L/(mol) for $K_{BF}$ suggests that when benzofuran is present, it absorbs strongly to the catalyst surface, thereby occupying many of the active sites. The average concentration of benzofuran in both sets of reactions (4:1 and 6:1 hydrogen to benzofuran) was approximately 0.01 M, so the value of the denominator in the expression for $k_{2,eff}$ is approximately 10. Thus, $k_{2,eff}$ is about 10% of the value of $k_2$ given in Table 3. This result fits well with the significant decrease observed in Section 3.3 in the direct deoxygenation reaction rate when starting with benzofuran.

These rate constants, $k_{2,eff}$ and $k_2$, indicate that the hydrogenolysis of ethylphenol to form ethylbenzene is the rate-limiting step in this reaction sequence when benzofuran is present because $k_{2,eff}$ is slowed significantly by benzofuran. A comparison of $k_5$ and $k_{2,eff}$ shows that inhibition by benzofuran on the direct deoxygenation pathway (reaction (2)) provides a basis for the difference in selectivity to deoxygenated products when starting with benzofuran and ethylphenol. Recall from Section 3.3 that the ethylphenol (3:1) and benzofuran (6:1) reactions produced very different ethylbenzene to ethylcyclohexane ratios of 11 and 1.7, respectively, at 25 min. When ethylphenol is the starting reagent, the effective direct deoxygenation rate constant ($k_{2,eff} = k_2 = 0.161\ L^2/(mol\ min\ g_{cat})$) is about four times the rate constant for ethylcyclohexanol deoxygenation ($k_5 = 0.0424\ L^2/(mol\ min\ g_{cat})$), thereby producing more ethylbenzene than ethylcyclohexane. When benzofuran is the starting reagent, the effective direct deoxygenation rate constant drops approximately an order of magnitude ($k_{2,eff} \approx 0.016\ L^2/(mol\ min\ g_{cat})$) while the ethylcyclohexanol deoxygenation rate constant ($k_5$) remains unchanged. This results in $k_5$ being about 2.5 times $k_{2,eff}$.

A comparison of the hydrogenation/dehydrogenation rate constants ($k_3$, $k_{-3}$, $k_4$, $k_{-4}$) shows that dehydrogenation of ethylcyclohexanone occurs more readily than the dehydrogenation of ethylcyclohexanol ($k_{-3}$ is about 6 times larger than $k_{-4}$). The rate constant for ethylcyclohexanone hydrogenation ($k_4$) is also the same magnitude as $k_1$ and $k_2$, indicating that

**Table 2**
Kinetics model of the major benzofuran reaction pathways shown in Fig. 8 at 380 °C and a 0.16 g/mL water density at reaction conditions. $W$ is the catalyst mass (gcat).

$$\frac{1}{w}\frac{dC_{BF}}{dt} = -k_1 C_{BF} C_{H2} \quad (3)$$

$$\frac{1}{w}\frac{dC_{BF}}{dt} = k_1 C_{BF} C_{H2} - \frac{C_{EP} C_{H2}(k_2+k_6)}{1+K_1 C_{BF}} - K_3 C_{EP} C_{H2}^2 + k_{-3} C_{ECHONE} \quad (4)$$

$$\frac{1}{w}\frac{dC_{BF}}{dt} = \frac{k_2 C_{EP} C_{H2}}{1+K_1 C_{BF}} \quad (5)$$

$$\frac{1}{w}\frac{dC_{ECHONE}}{dt} = k_3 C_{EP} C_{H2}^2 - k_{-3} C_{ECHONE} - k_4 C_{ECHONE} C_{H2} + k_{-4} C_{ECHOL} \quad (6)$$

$$\frac{1}{w}\frac{dC_{ECHONE}}{dt} = k_4 C_{EP} C_{H2} - k_{-4} C_{ECHOL} - k_5 C_{ECHOL} C_{H2} \quad (7)$$

$$\frac{1}{w}\frac{dC_6}{dt} = k_5 C_{ECHOL} C_{H2} \quad (8)$$

$$\frac{1}{w}\frac{dC_{H2}}{dt} = -2k_1 C_{BF} C_{H2} - \frac{C_{EP} C_{H2}(k_2+k_6)}{1+K_1 C_{BF}} - 2k_3 C_{EP} C_{H2}^2 + 2k_{-3} C_{ECHONE} - k_4 C_{EP} C_{H2} + k_{-4} C_{ECHOL} - k_5 C_{ECHOL} C_{H2} \quad (9)$$

**Table 3**
Optimized values of the rate constants in Fig. 8.

| $k_1^*$ | $k_2^*$ | $k_3^{**}$ | $k_{-3}^{\#}$ | $k_4^*$ | $k_{-4}^{\#}$ | $k_5^*$ | $k_6^*$ | $K_{BF}^{\#\#}$ |
|---|---|---|---|---|---|---|---|---|
| 0.146 | 0.161 | 0.501 | 0.338 | 0.0934 | 0.0580 | 0.0424 | 0.0554 | 965 |

Units: $^*L^2/(\text{mol min } g_{cat})$, $^{**}L^3/(\text{mol}^2 \text{ min } g_{cat})$, #L/(min $g_{cat}$), ##L/(mol).

ethylcyclohexanone can be readily hydrogenated under these reaction conditions.

### 3.4.3. Model analysis

The optimized kinetic model accurately correlates the concentration of each reaction species as shown in Figs. 1, 2, 6 and 7. In general, the kinetic model captures the trends in the experimental data and is within the experimental error bars (standard deviations). A more detailed comparison of the fit of the kinetic model to the experimental data is examined in Section 3.4.4. The kinetic model is also useful for understanding how process variables affected the product distribution, and it provides insights into the reaction network not observed solely from the experimental data. We elaborate on these points below.

*3.4.3.1. Benzofuran.* Figs. 1 and 2 show the fit of the kinetic model to the experimental data for the benzofuran reactions. The kinetic model captured the increase in ethylcyclohexanone concentration at the higher hydrogen loading by using a second order dependence on hydrogen for the ethylphenol hydrogenation reaction. A rate equation that was first order in hydrogen was not capable of fitting the data. This hydrogenation step is the only one in the kinetic model that has a reaction order higher than unity for a given reactant. This second order dependence is important for capturing the change in deoxygenated product distribution at the higher hydrogen loading because the only route to produce ethylcyclohexane begins with the hydrogenation of ethylphenol to produce ethylcyclohexanone, as shown in Fig. 8. The higher hydrogen loading doubles the rate of ethylphenol hydrogenation to ethylcyclohexanone from 0.012 to 0.024 mol/(min $g_{cat}$) at 15 min, thereby allowing for the formation of ethylcyclohexane. The second order dependence on hydrogen for this hydrogenation reaction means that very little (<0.008 M) ethylcyclohexanone and ethylcyclohexane are produced at the 4:1 hydrogen to benzofuran molar ratio.

Further examination of Fig. 2 reveals that the kinetic model suggests that the concentration of ethylcyclohexanone increases rapidly before reaching a maximum at approximately 5 min, and then is partially consumed before the first experimental data point was taken at 10 min. The appearance of 0.014 M ethylcyclohexane at 10 min in the experimental data necessitates this behavior in the kinetic model because the formation ethylcyclohexane requires that the ethylcyclohexanone and ethylcyclohexanol reactions proceed rapidly.

*3.4.3.2. Ethylphenol.* Fig. 6 shows the fit of the kinetic model to the experimental data for the ethylphenol reactions. The experimental data and model show that the concentration of ethylphenol decreases rapidly and is primarily directly deoxygenated to ethylbenzene. The limited production of ethylcyclohexane is a result of the limited hydrogenation of ethylphenol to produce ethylcyclohexanone. The model suggests that the concentration of ethylcyclohexanone increases rapidly, and then is mostly consumed within 10 min. The majority of the ethylcyclohexanone is dehydrogenated back to ethylphenol while a smaller amount is converted to ethylcyclohexanol. The majority of the ethylcyclohexanol produced is deoxygenated to ethylcyclohexane.

Comparing the calculated ethylcyclohexanone concentrations in Figs. 2 and 6 reveals that ethylcyclohexanone is consumed more rapidly when ethylphenol, rather than benzofuran, is the starting reactant. This result is evident from the rapid decrease in the calculated ethylcyclohexanone concentration from its maximum in Fig. 6 and comparing it to the gradual decrease from its maximum in Fig. 2. The slower decrease in Fig. 2 is a result of the direct deoxygenation pathway being inhibited by the presence of benzofuran, as discussed in Section 3.4.2.

*3.4.3.3. Ethylcyclohexanol.* Fig. 7 shows the temporal variation in the concentration of the major products for reactions at 380 °C with a 0.5 to 1 hydrogen to ethylcyclohexanol ratio. The model captures the high conversion (79 ± 9% at 10 min) and the concentration of the major reaction products. Interestingly, the major deoxygenation product was ethylbenzene even at short reaction times (10 min). An analysis of the rate constants in the previous section indicated that ethylbenzene is the major deoxygenated product because the hydrogenation/dehydrogenation reactions between ethylphenol, ethylcyclohexanone, and ethylcyclohexanol occur rapidly. Furthermore, when compared to the benzofuran reactions in Fig. 2, the experimental and model results for the ethylcyclohexanol reactions in Fig. 7 show significantly lower concentrations of ethylphenol and ethylcyclohexanone at all reaction times even though the reaction network (Fig. 8) shows that ethylcyclohexanone and ethylphenol must be formed before producing ethylbenzene. The reason for the lower ethylphenol and ethylcyclohexanone concentrations is that without benzofuran present, the direct deoxygenation of ethylphenol occurs quickly, thereby keeping the concentration of ethylphenol and subsequently ethylcyclohexanone low.

### 3.4.4. Comparison of experimental and calculated results

Table 4 shows the error (Eq. (2)), normalized for the number of data points, for each data set that was fit to the kinetic model, along with the total error. The values in this table indicate that the error per data point was distributed fairly evenly across all of the data sets, suggesting that the model is not favoring one data set over another.

Fig. 9 shows a parity plot for all of the data fit with the kinetic model. This plot has scatter about the diagonal parity line, but it appears to be free of systematic deviations from the parity line. Furthermore, error bars of one standard deviation encompassed the parity line in most cases. This outcome indicates that the model adequately describes the data with the experimental error. The deviations from the parity line may be due to several factors. First, the adsorption equilibrium constants of reaction species other than benzofuran might play roles in the reaction rates, but these terms

**Table 4**
Tabulation of normalized error between the kinetic model calculations and the experimental data for the concentration of each reaction species. The errors are normalized by the number of data points.

| Model | Error $(\text{mol}^2/\text{L}^2) \times 10^3$ |
|---|---|
| 4:1 Benzofuran | 4.54 |
| 6:1 Benzofuran | 3.50 |
| 0.5:1 Ethylcyclohexanol | 4.20 |
| 3:1 Ethylphenol | 1.78 |
| Total | 14.02 |

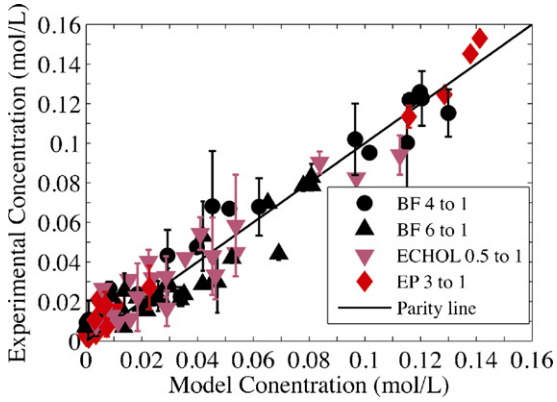


**Fig. 9.** Parity plot for the kinetic model.

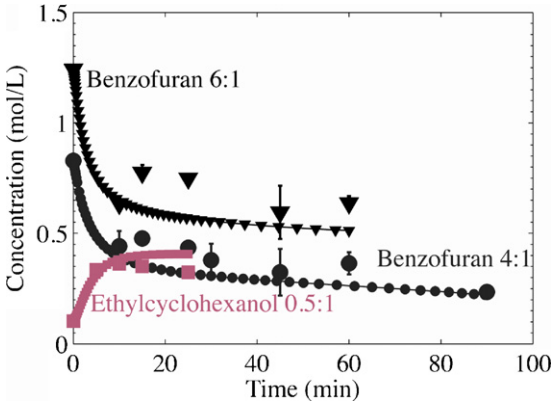


**Fig. 11.** Concentration of hydrogen from experiments and the kinetic model prediction.

were omitted for simplicity in this model. Second, the reaction orders for hydrogen and the organic reactants may differ slightly from those used in this model. We did examine a variety of integer reaction orders, and the present model provided the best results. It may be possible, however, that a better fit could be obtained with a non-integer reaction order.

### 3.4.5. Model validation

To validate the kinetic model presented above, we predicted the temporal variation of the concentrations of major products when benzofuran was reacted at a 4:1 hydrogen to benzofuran molar ratio with only 5 mg of the Pt/C (as opposed to the 10 mg used in Fig. 1). Fig. 10, which shows these results, indicates that at this lower catalyst loading, the model accurately predicts the experimental concentration for each major product. This result provides further evidence that the model accurately captures the phenomena occurring in the reactor during the hydrothermal catalytic deoxygenation of benzofuran.

### 3.4.6. Hydrogen consumption

Recent related research in our lab showed that catalytic deoxygenation reactions (of fatty acids) can occur in water without added hydrogen [20,21]. This observation led to speculation that water may be able to donate hydrogen to perform deoxygenation. If water were a major contributor of hydrogen to the present reaction, the experimental hydrogen concentrations should be consistently higher than the concentrations present if the hydrogen gas loaded into the reactor were the sole hydrogen source. We used the kinetic model, in which all H atoms are supplied by the hydrogen gas, to calculate these hydrogen concentrations. Note that the

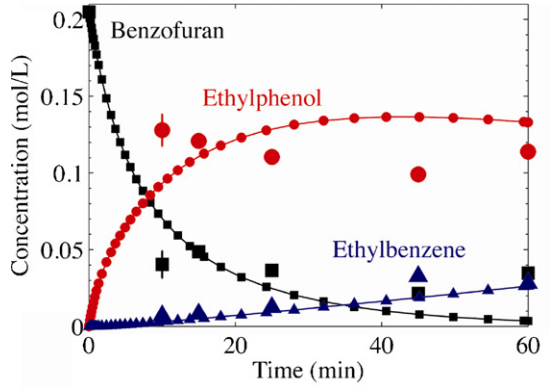


**Fig. 10.** Experimental results and model predictions for the major products from benzofuran at 380 °C with a 4:1 hydrogen to benzofuran molar ratio and 5 mg of 5 wt% Pt/C.

experimental hydrogen concentrations were not used to determine the model parameters, so the model calculations for the hydrogen concentrations are predictions and not a correlation of results.

Fig. 11 shows that the model predicts the experimental concentration of hydrogen with reasonable accuracy, especially at the lower hydrogen loadings (benzofuran 4:1 and ethylcyclohexanol 0.5:1). Moreover, the hydrogen concentrations clearly decrease significantly from their initial values in the benzofuran experiments. These results indicate that water is likely not a major contributor of hydrogen for these reactions. Reactions for 30 min with benzofuran under a helium atmosphere had only a $16.2 \pm 0.5\%$ conversion and less than 1% deoxygenation, confirming this hypothesis.

### 3.5. Diffusion limitations

Although a wrist action shaker continuously agitated the reactors during the experiments, we wanted to be certain we were measuring the intrinsic reaction kinetics. To test for the possibility of pore diffusion limitations, the Weisz-Prater parameter, $C_{wp}$, was calculated. $C_{wp}$ values less than unity indicate that the reaction is under kinetic control and pore diffusion limitations are negligible [29].

$$C_{wp} = \frac{-r(\text{obs})R^2}{D_e C_{AS}} \tag{10}$$

$C_{AS}$, the concentration of reactant at the catalyst surface, was taken to be the initial bulk benzofuran concentration (0.21 mol/L). Fu et al. obtained $R$, the radius of the catalyst particle, from the catalyst manufacturer as $2.5 \times 10^{-3}$ cm [20]. $D_{AB}$, the diffusivity of benzofuran in supercritical water at 380 °C and 4200 psig, was estimated to be $1.5 \times 10^{-3}$ cm$^2$/s from the empirical equation developed by Fuller, Schettler, and Giddings [30]. This estimate accounts for the temperature and pressure at reaction conditions, and molecular structure of water and benzofuran. The effective diffusivity, $D_e$, was then calculated ($1.6 \times 10^{-4}$ cm$^2$/s) using the same scaling factor as Fu et al. to account for the porosity and tortuosity of the catalyst particle [20]. The initial observed rate, $-r$(obs) was calculated at 380 °C from the model as 0.08 mol/L s. These values led to a $C_{wp}$ value of 0.01, indicating this reaction is kinetically controlled under the conditions investigated.

## 4. Conclusion

Pt/C (5 wt%) was an effective catalyst for the deoxygenation of benzofuran in supercritical water. Examination of process variables revealed new methods to tune product selectivities to favor either aromatic or hydrogenated deoxygenated products. Not surprisingly, decreasing the hydrogen loading decreased the selectivity to

fully hydrogenated products, but more surprisingly, so did increasing the water loading. The results from these experiments and others, as outlined above, led to the development of a reaction network for benzofuran. During the development of the reaction network, we found that phenols inhibited the hydrogenation of ethylbenzene and the dehydrogenation of ethylcyclohexane, and that the rate equation for hydrogenation of ethylphenol is highly dependent (reaction order > 1) on the concentration of hydrogen. Last, we developed and validated a kinetic model that included benzofuran inhibiting the direct deoxygenation of ethylphenol to ethylbenzene. This model was also used to determine that water is unlikely to be a major source of hydrogen for the reactions described herein, as was previously speculated for the deoxygenation of fatty acids [20].

## Acknowledgements

J.G. Dickinson acknowledges financial support from a NSF Graduate Research Fellowship. We gratefully acknowledge the National Science Foundation (Grant EFRI-0937992) and the College of Engineering for their financial support.

## Appendix A. Supplementary data

Supplementary data associated with this article can be found, in the online version, at http://dx.doi.org/10.1016/j.apcatb.2012.05.005.

## References

[1] P. Biller, A.B. Ross, Bioresource Technology 102 (2010) 215–225.
[2] T.M. Brown, P. Duan, P.E. Savage, Energy and Fuels 24 (2010) 3639–3646.
[3] P. Duan, P.E. Savage, Industrial and Engineering Chemistry Research 50 (2011) 52–61.
[4] S. Inoue, Y. Dote, S. Sawayama, T. Minowa, T. Ogi, S. Yokoyama, Biomass and Bioenergy 6 (1994) 269–274.
[5] U. Jena, K.C. Das, J.R. Kastner, Bioresource Technology 102 (2011) 6221–6229.
[6] T. Matsui, A. Nishihara, C. Ueda, M. Ohtsuki, N. Ikenaga, T. Suzuki, Fuel 76 (1997) 1043–1048.
[7] T. Minowa, S. Yokoyama, M. Kishimoto, T. Okakura, Fuel 74 (1995) 1735–1738.
[8] A.B. Ross, P. Biller, M.L. Kubacki, H. Li, A. Lea-Langton, J.M. Jones, Fuel 89 (2010) 2234–2243.
[9] S. Sawayama, T. Minowa, S.Y. Yokoyama, Biomass and Bioenergy 17 (1999) 33–39.
[10] P.J. Valdez, J.G. Dickinson, P.E. Savage, Energy and Fuels 25 (2011) 3235–3243.
[11] Y.F. Yang, C.P. Feng, Y. Inamori, T. Maekawa, Resources, Conservation and Recycling 43 (2004) 21–33.
[12] P. Duan, P.E. Savage, Bioresource Technology 102 (2010) 1899–1906.
[13] P. Duan, P.E. Savage, Energy & Environmental Science 4 (2011) 1447–1456.
[14] P. Duan, P.E. Savage, Applied Catalysis B: Environmental 104 (2011) 136–143.
[15] E.L. Kunkes, D.A. Simonetti, R.M. West, J.C. Serrano-Ruiz, C.A. Gärtner, J.A. Dumesic, Science 322 (2008) 417.
[16] T.P. Vispute, G.W. Huber, Green Chemistry 11 (2009) 1433–1445.
[17] T.P. Vispute, H. Zhang, A. Sanna, R. Xiao, G.W. Huber, Science 330 (2010) 1222–1227.
[18] J.W. Medlin, ACS Catalysis 1 (2011) 1284–1297.
[19] P. Duan, P.E. Savage, Applied Catalysis B: Environmental 108–109 (2011) 54–60.
[20] J. Fu, X. Lu, P.E. Savage, Energy & Environmental Science 3 (2010) 311–317.
[21] J. Fu, X. Lu, P.E. Savage, ChemSusChem 4 (2011) 481–486.
[22] A.Y. Bunch, U.S. Ozkan, Journal of Catalysis 206 (2002) 177–187.
[23] A.Y. Bunch, X. Wang, U.S. Ozkan, Journal of Molecular Catalysis A: Chemical 270 (2007) 264–272.
[24] C.L. Lee, D.F. Ollis, Journal of Catalysis 87 (1984) 325–331.
[25] Y. Romero, F. Richard, Y. Renème, S. Brunet, Applied Catalysis A-General 353 (2009) 46–53.
[26] D.C. Elliott, L.J. Sealock Jr., E.G. Baker, Industrial and Engineering Chemistry Research 32 (1993) 1542–1548.
[27] A. Vargas, T. Burgi, A. Baiker, Journal of Catalysis 222 (2004) 439–449.
[28] M.C. Edelman, M.K. Maholland, R.M. Baldwin, S.W. Cowley, Journal of Catalysis 111 (1988) 243–253.
[29] H.S. Fogler, Elements of Chemical Reaction Engineering, Prentice Hall, Westford, 2008.
[30] E.N. Fuller, P.D. Schettler, J.C. Giddings, Industrial and Engineering Chemistry Research 58 (1966) 18–27.